ORIGINAL ARTICLE

Influence of double rods and interbody cages on quasistatic range of motion of the spine after lumbopelvic instrumentation

Yves Ntilikina[1,2] · Yann Philippe Charles[2] · Sylvain Persohn[1] · Wafa Skalli[1]

Abstract

Purpose This in vitro biomechanical study compares residual lumbar range of motion (ROM) and rod strain after lumbopelvic instrumentation using 2 rods, 4 rods and interbody cages.

Methods Seven human cadaveric specimens were instrumented from L1 to sacrum, and pelvic screws were implanted. The pelvis was constrained and moments up to 7.5 Nm were applied to T12. Segmental L1–S1 ROM was analyzed by tracking radiopaque balls implanted in each vertebra using biplanar radiographs. Deformation within principal rods was measured by strain gauges. Four configurations were compared: 2 rods (2R), 4 rods (4R), 4 rods + ALIF at L4–L5 and L5–S1 (4R + ALIF), 2 rods + ALIF (2R + ALIF).

Results Intact average global L1–S1 ROM was 42.9° (27.9°–66.0°) in flexion–extension (FE), 35.2° (26.8°–51.8°) in lateral bending (LB), 18.6° (6.7°–47.8°) in axial rotation (AR). In FE, average ROM was 1.9° with both 4-rod configurations versus 2.5° with 2R and 2.8° with 2R + ALIF ($p < 0.05$). In LB, ROM ranged between 1.2° and 1.5° without significant differences. In AR, ROM was 2.5° with both 4-rod configurations versus 2.9° with 2R ($p = 0.07$) and 3.1° with 2R ALIF ($p = 0.01$). In FE, strain decreased by 64% and 65% in principal rods at L3–L4 with 4-rod. When comparing 2-rod configurations, strain decreased by 1% in flexion and increased by 22% in extension at L3–L4 when adding an ALIF at L4–L5 and L5–S1.

Conclusions Double rods and interbody cages decrease residual ROM in FE and AT. Double rods seem efficient in limiting strain in principal rods. The use of single rods with cages at the lumbosacral junction increases strain at the first adjacent level without cage.

Keywords Spinal deformity · Pelvic fixation · Double rod instrumentation · Anterior lumbar interbody fusion · Biomechanics · Lumbosacral range of motion · Rod strain

Introduction

Degenerative lumbar scoliosis and sagittal malalignment represent common spinal deformities in the aging population. Adult spinal deformity (ASD) associated with imbalance has an impact on health-related quality of life (QoL) [1, 2]. Surgical treatment might be considered if conservative treatment remains inefficient on low back and leg pain, and in progressive trunk imbalance. Although surgical treatment of ASD improves QoL, the incidence of long-term mechanical complications is reported between 30 and 40% [3, 4]. These rates increase if the spinal deformity and degenerative changes require instrumentation to the sacrum [5–7]. Among failures related to long instrumentation including the lumbosacral junction, distal screw loosening represents a common problem. In vitro biomechanical tests have demonstrated that an additional pelvic fixation has the highest potential to protect the S1-anchorage [8]. Nevertheless, the use of strong iliac seems to be associated with an increased rate of rod fractures [9, 10]. Implant failure like rod breakage often indicates the presence of pseudarthrosis, which can lead to revision surgery.

It appears that posterolateral fusion might not be sufficient when instrumenting the thoracolumbar spine including the sacrum and pelvis. A rigid pelvic fixation might lead to fatigue of lumbar instrumentation under cyclic loading

✉ Yves Ntilikina
  yves.ntilikina@chru-strasbourg.fr

1 Institut de Biomécanique Humaine Georges Charpak, Arts et Métiers ParisTech, 151, Boulevard de l'Hôpital, 75013 Paris, France

2 Service de Chirurgie du Rachis, Hôpitaux Universitaires de Strasbourg, Strasbourg, France

(daily activities, walking and recurrent anterior malalignment) which increases the risk of pseudarthrosis and rod fracture. Therefore, an anterior column support and fusion using interbody cages might be recommended to avoid pseudarthrosis [11–13]. First clinical studies suggest that multiple rod constructs could reduce the incidence of pseudarthrosis [14–18]. Figure 1 illustrates a clinical case of degenerative lumbar scoliosis instrumented with a 4-rod construct and additional interbody cages.

The main hypothesis of this study is that the use of interbody cages and/or multiple rods could decrease residual minimal range of motion in the instrumented segment, which might lead to nonunion and implant failure on long term.

The purpose of this biomechanical study was to investigate residual mobilities within the entire lumbar spine and strain in the rods after lumbosacral and pelvic instrumentation using single rods, double rods and interbody cages.

Materials and methods

Specimens

Seven fresh-frozen human cadaveric T12-pelvis specimens were tested. Specimens without spinal pathologies that would influence biomechanical testing (osteoporosis, fractures, metastases, major decrease in intervertebral disk height or facet joint osteoarthritis) were selected by visual examination and computed tomography (CT). All donors were males, and their average age was 57.7 (42–63) years. The average bone mineral density was 104.2 mg/cm³.

The specimens were freshly dissected, sealed in double plastic bags, frozen and stored at −20 °C until testing. The specimens were thawed to 6 °C for 12–14 h before starting the preparation process. The experiment itself was performed at room temperature. Soft tissues were removed, leaving all ligaments, joint capsules, disks and bony structures intact.

After reconstruction of the specimen's geometry from three-dimensional (3D) CT images (Medical imaging interaction toolkit, MITK 2016.11, Heidelberg, Germany), specimen-specific custom-made molds were 3D-printed to constrain the T12 vertebral body and spinous process cranially and the ischium caudally. The bone–mold interface was additionally secured with small screws. Two-millimeter-diameter stainless steel balls were then implanted in the cortical bone from L1 to S1 after drilling a small pilot hole (one in each spinous process and four in each vertebral body). Six balls were implanted in the sacrum and three in each iliac wing. Figure 2 shows anterior–posterior and lateral radiographs (EOS™, EOS Imaging, Paris, France) that allowed calculating 3D positions of the balls using
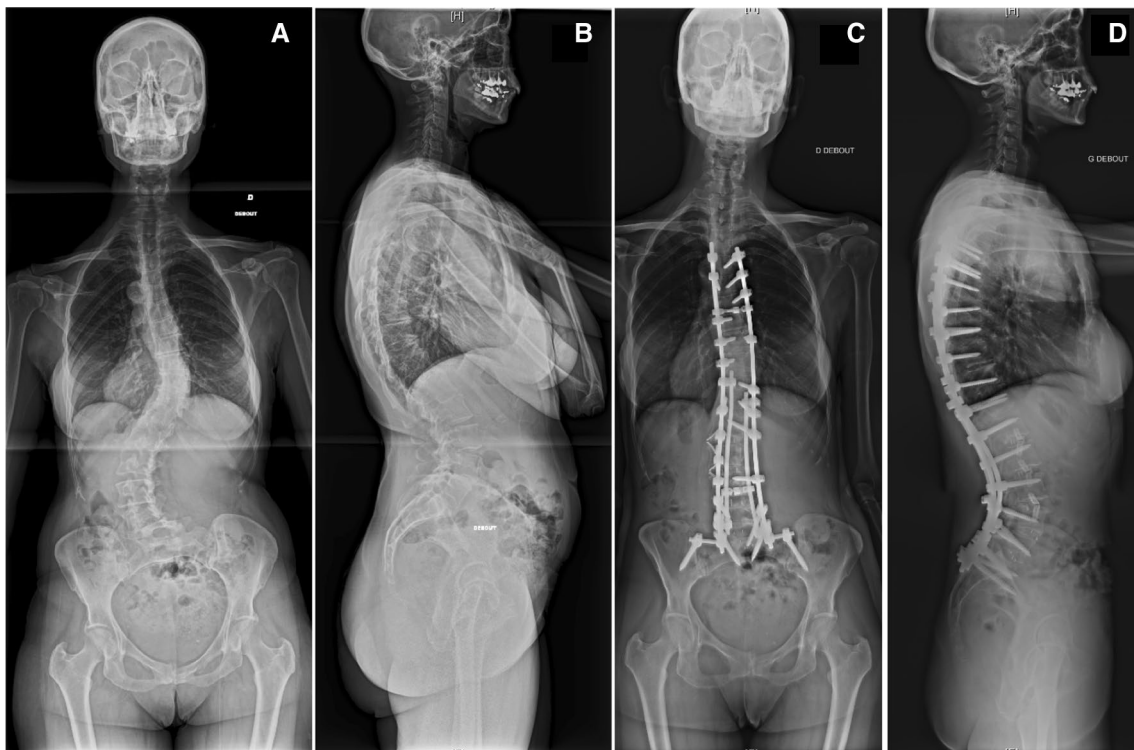
Fig. 1 Preoperative posterior–anterior (**a**) and lateral (**b**) full spine standard radiographs of a patient with adult scoliosis and postoperative posterior–anterior (**a**) and lateral (**b**) radiographs after T5-ilium instrumentation using double rods and interbody fusion cages

Fig. 2 Anteroposterior (**a**) and lateral (**b**) biplanar radiographs of an intact specimen showing cranial and caudal custom molds (black arrows) and metallic balls in each vertebra from L1 to S1, the sacrum and pelvis
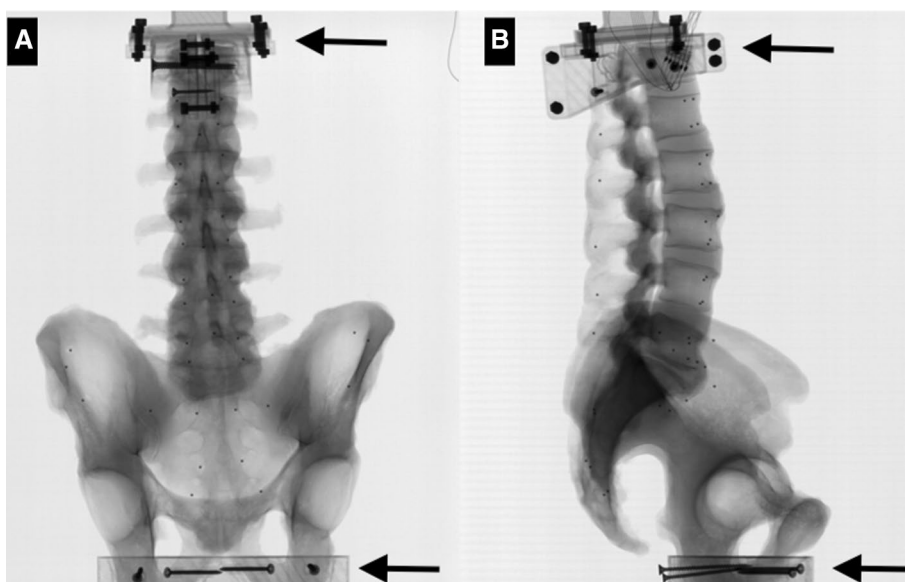
MATLAB software (MathWorks, Natick, MA, USA). The coordinate systems for each group of balls (RBi) were associated with the respective vertebrae [19], the sacrum and pelvis [20–22]. The global coordinate system of the EOS cabin was defined as R0. The transformation matrices for each RBi to the global R0 allowed calculating relative successive positions between vertebrae and sacrum.

Kinematic testing

The flexibility tests were conducted in a specific spine-testing device. The pelvic 3D-printed mold was rigidly fixed to the pelvis and to a frame in the EOS™ system. The cranial mold, fixed on T12, was mounted to a motor (Gearmotor 3242G024C, Faulhaber SAS, Montigny-le-Bretonneux, France), which was unconstrained in the three directions of translation and two perpendicular axes of rotation (Fig. 3). This system allowed applying quasistatic moments for flexion–extension, lateral bending and axial torsion by gradual loading in steps of 1.5 Nm, with an interval of 15 s between each step, until a maximum of 7.5 Nm was reached [23]. Three preloading cycles were performed to compensate for small viscoelastic effects. A 6-axis load cell (FTD-Gamma SI-130-10, ATI Industrial Automation, Apex, NC, USA) placed under the specimen allowed checking whether pure moments were applied. After three preconditioning cycles, flexion and extension were completed during the same loading–unloading cycle. The same applied for right and left lateral bending as well as right and left axial torsion. Biplanar radiographs were taken at each increment, to track the metal balls. The successive positions of these markers were measured during the loading–unloading cycle values, which allowed to determine three angular displacements (rotations around X, Y and Z axis) and three linear displacements
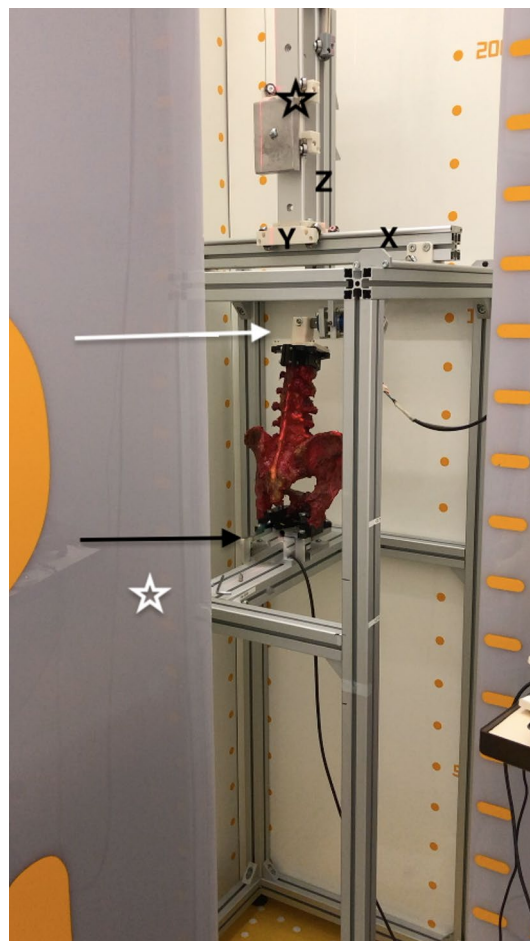
Fig. 3 Intact specimen mounted in the test bench in the biplanar X-rays system (white star) with the motor linked to the T12 mold by a universal joint (white arrow), the 6-axis sensor below the specimen (black arrow), the balancing weight above the motor (black star)

(translations along TX, TY and TZ). The centers of the metal markers were localized automatically with template-matching using normalized cross-correlation. The incertitude (95% confidence interval) of this motion tracking method was estimated using a motorized linear translation stage and was below 0.049 mm for each axis.

Load–displacement curves were obtained, thus quantifying 3D segmental range of motion (ROM) between vertebrae and sacrum for the noninstrumented specimen. The global ROM of L1 related to the sacrum was considered for instrumented configurations.

The uncertainty of mobility measurement was estimated using a Monte Carlo method introducing Gaussian noise to the different sources of possible errors and performing 300 simulations. The confidence interval (95% CI) was lower than 0.12° for the main rotations, 0.23° for coupled rotations and 0.12 mm for linear displacements.

Instrumentation configurations

An orthopedic spine surgeon performed all instrumentations (Erisma Deformity®, Clariance, Beaurains, France) using the free-hand technique for pedicle screw placement. Polyaxial pedicle screws were placed bilaterally from L1 to L5 (6.5 mm diameter, 45 mm length) and at S1 (7.5 mm diameter, 45 mm length). Iliac screws (8.5 mm diameter, 70 mm length) were placed bilaterally in a subcrestal fashion. Cobalt–chromium rods (CoCr, 5.5 mm diameter) were contoured and connected to the screws while taking care to

minimize the need for reduction techniques. Offset connectors between iliac screws and rods were utilized. A crosslink connector was placed between L5 and S1 screws. Two uni-axial strain gauges (KFG-2N-120-C1-11 L3M2R, KYOWA, Tokyo, Japan) were stuck on the posterior side of each rod midway between L3 and L4 screws (Fig. 4). This positioning allowed rod strain measurements in flexion–extension.

This standard setting of posterior L1-pelvis instrumentation was defined as 2-rod configuration (2R). Afterward, two additional 5.5-mm-diameter CoCr rods were placed medially and connected to the principal rods between L1 and L2 and between the S1 and iliac screws using side-by-side connectors, which was defined as 4-rod configuration (4R). An anterior discectomy was then performed at L4–L5 and L5–S1 while preserving the endplates and the posterior longitudinal ligament. Anterior lumbar interbody fusion (ALIF) polyether-ether-ketone (PEEK) cages were then inserted at both levels. The cage height (10–14 mm) was adapted to each level in order to fill out the interbody space (4R + ALIF configuration). The accessory rods were then removed for the last step, which represented a 2-rod construct with L4–L5 and L5–S1 ALIF cages (2R + ALIF configuration). Figure 5 shows radiographs for each configuration.

Segmental ROM was measured between L1 and S1 in flexion and extension, left and right lateral bending and axial torsion for each instrumentation configuration. Configurations were then compared to the intact specimen, and results were reported as percentage using the formula: variation = ROM instrumented − ROM intact/ROM intact × 100.

Fig. 4 Posterior view of a specimen with 4-rod instrumentation and custom mold fixation (arrows) at T12 and the pelvis (**a**). Focus on strain gauges (white circles) placed on the principal rods between the pedicle screws of L3 and L4 (**b**)
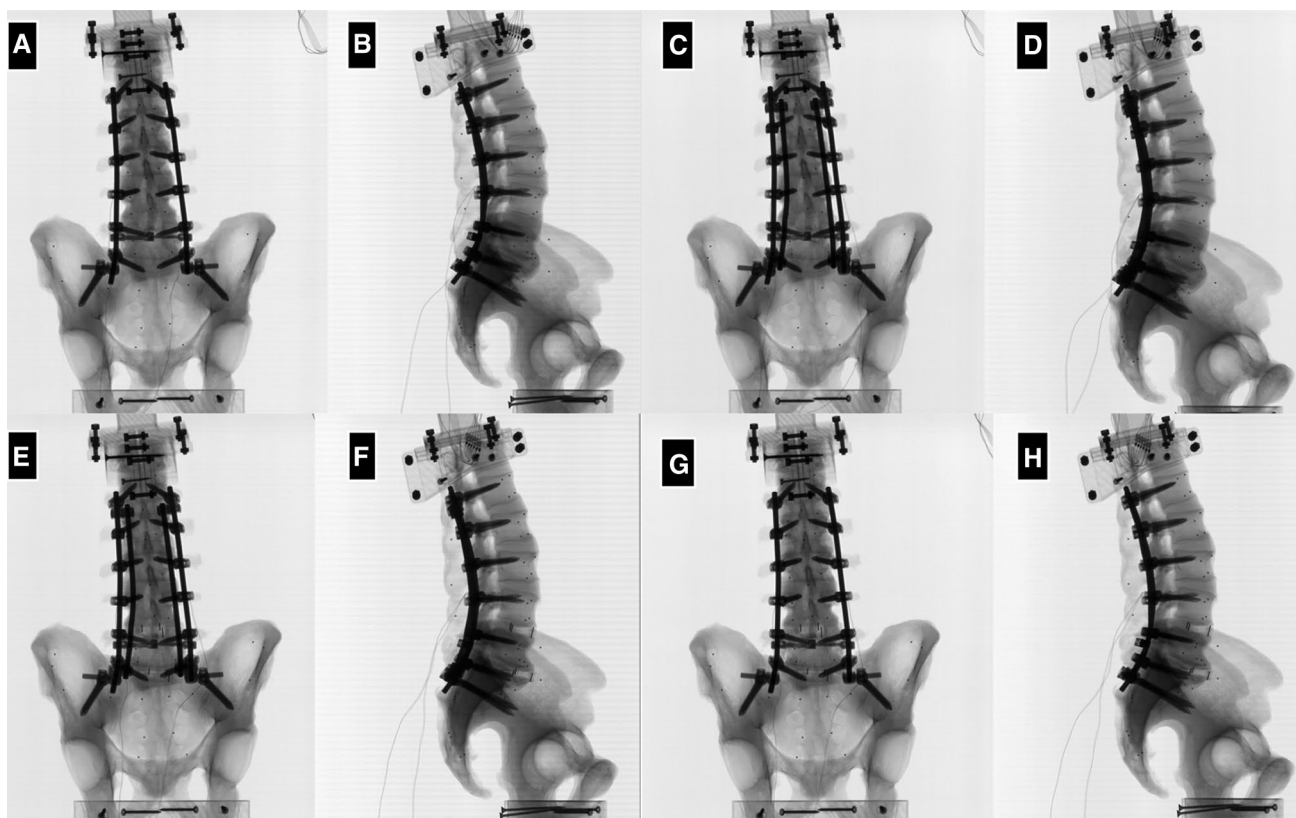
Fig. 5 Biplanar radiographs of the four instrumented configurations: 2 rods (**a**, **b**), 4 rods (**c**, **d**), 4 rods + ALIF L4–L5 and L5–S1 (**e**, **f**), 2 rods + ALIF L4–L5 and L5–S1 (**g**, **h**)

The strain in the principal rods was measured by strain gauges for each configuration between L3 and L4 in flexion–extension only.

Statistical analysis

Data were analyzed using R software (R Foundation, Vienna, Austria). Quantitative data were expressed as average, standard deviation and range. A Shapiro–Wilk test was used to check normal distribution. A linear mixed model was then used to analyze quantitative variables with a fixed effect (configuration) and a random effect (specimen). ROM was compared between the intact specimen and each instrumented configuration. Rod strain was compared between instrumented configurations. The significance level was set at $p < 0.05$.

Results

Segmental lumbar range of motion

Table 1 demonstrates segmental ROM which was measured when a 7.5 Nm bending moment was applied to the

Table 1 Segmental lumbar range of motion in intact specimens: average values ± standard deviation (minimum–maximum)

Level	Flexion–extension	Lateral bending	Axial rotation
L1–L2	7.4° ± 1.7° (4.4°–9.6°)	7.9° ± 2.1° (6.0°–11.3°)	2.8° ± 1.4° (1.2°–4.6°)
L2–L3	7.7° ± 2.8° (4.1°–13°)	9.5° ± 2.7° (6.7°–13.1°)	4.9° ± 3.7° (1.1°–11.9°)
L3–L4	7.4° ± 1.8° (5.0°–10.7°)	9.7° ± 1.8° (8.0°–11.8°)	5.0° ± 3.0° (1.2°–10.4°)
L4–L5	10.2° ± 3.6° (4.9°–15.7°)	10.3° ± 2.9° (5.7°–13.8°)	5.8° ± 5.3° (1.2–10.4)
L5–S1	10.1° ± 6.0° (2.6°–17.6°)	6.0° ± 3.8° (1.1°–10.2°)	2.0° ± 2.3° (0.6°–7.0°)

intact lumbar specimens. ROM ranged from 7.4° to 10.5° in flexion–extension, 6.0° to 10.3° in lateral bending and 2.0° to 5.8° in axial torsion. The largest ROM was found at the level L4–L5 for each direction.

The segmental ROM with instrumentation is described in Table 2.

Table 2 Segmental lumbar range of motion in instrumented specimens: average values ± standard deviation (minimum–maximum)

		L1–L2	L2–L3	L3–L4	L4–L5	L5–S1
2R	FE	0.7°±0.3° (0.3°–1.3°)	0.4°±0.2° (0.2°–0.6°)	0.4°±0.1° (0.2°–0.6°)	0.6°±0.2° (0.4°–0.9°)	0.8°±0.5° (0.3°–1.9°)
	LB	1.2°±0.6° (0.7°–2.5°)	0.4°±0.2° (0.1°–0.6°)	0.2°±0.1° (0.1°–0.4°)	0.2°±0.1° (0.1°–0.4°)	0.3°±0.1° (0.2°–0.4°)
	AR	1.1°±0.4° (0.6°–1.7°)	0.8°±0.4° (0.4°–1.3°)	0.8°±0.4° (0.4°–1.7°)	0.6°±0.2° (0.6°–0.9°)	0.6°±0.3° (0.3°–1.2°)
4R	FE	0.8°±0.4° (0.4°–1.5°)	0.4°±0.2° (0.1°–0.9°)	0.3°±0.2° (0.1°–0.7°)	0.5°±0.3° (0.2°–1.1°)	0.7°±0.4° (0.3°–1.6°)
	LB	1.4°±0.8° (0.8°–3°)	0.4°±0.2° (0.2°–0.7°)	0.4°±0.2° (0.1°–0.8°)	0.4°±0.2° (0.1°–0.7°)	0.4°±0.2° (0.1°–0.6°)
	AR	0.9°±0.4° (0.6°–1.8°)	0.8°±0.3° (0.4°–1.2°)	0.7°±0.3° (0.4°–1.4°)	0.5°±0.2° (0.3°–0.8°)	0.4°±0.1° (0.3°–0.7°)
4R + ALIF	FE	0.8°±0.4° (0.4°–1.5°)	0.5°±0.4° (0.1°–1.3°)	0.4°±0.3° (0.1°–0.8°)	0.5°±0.3° (0.2°–0.9°)	0.7°±0.2° (0.3°–1.0°)
	LB	1.4°±0.7° (0.9°–2.9°)	0.4°±0.2° (0.1°–0.8°)	0.5°±0.2° (0.1°–0.8°)	0.3°±0.2° (0.1°–0.6°)	0.4°±0.1° (0.2°–0.5°)
	AR	1.0°±0.3° (0.7°–1.6°)	0.8°±0.5° (0.3°–1.6°)	0.7°±0.2° (0.5°–1.0°)	0.5°±0.2° (0.3°–0.8°)	0.4°±0.1° (0.3°–0.6°)
2R + ALIF	FE	0.9°±0.5° (0.4°–1.7°)	0.5°±0.3° (0.3°–1.1°)	0.6°±0.4° (0.3°–1.4°)	0.7°±0.4° (0.3°–1.5°)	0.7°±0.2° (0.3°–0.9°)
	LB	1.5°±0.8° (0.7°–3.1°)	0.3°±0.1° (0.1°–0.6°)	0.3°±0.2° (0.1°–0.5°)	0.3°±0.2° (0.1°–0.7°)	0.3°±0.1° (0.1°–0.6°)
	AR	1.2°±0.5° (0.8°–2.3°)	0.9°±0.5° (0.4°–1.8°)	0.8°±0.4° (0.5°–1.5°)	0.5°±0.2° (0.3°–0.8°)	0.6°±0.2° (0.4°–1.0°)

FE, flexion–extension; LB, lateral bending; AR, axial rotation

Table 3 Global lumbar (L1–S1) range of motion for the intact spine and four instrumented configurations: average values ± standard deviation (minimum–maximum)

Configuration	Flexion–extension	Lateral bending	Axial rotation
Intact spine	42.9°±3.1° (27.9°–66.0°)	35.2°±3.2° (26.8°–51.8°)	18.6°±6.3° (6.7°–47.8°)
2 rods	2.5°±0.6° (1.2°–3.7°)*,†	1.2°±0.1° (1.2°–4.6°)*	2.9°±0.1° (1.7°–5.8°)#
4 rods	1.9°±0.3° (1.1°–3.2°)*,‡	1.4°±0.2° (0.7°–2.9°)*	2.5°±0.3° (1.5°–4.5°)#,‡
4 rods + ALIF	1.9°±0.1° (1.5°–2.9°)*,‡	1.3°±0.2° (0.6°–3.2°)*	2.5°±0.2° (1.7°–4.4°)#,‡
2 rods + ALIF	2.8°±0.3° (1.6°–4.1°)*,†	1.5°±0.2° (0.6°–3.5°)*	3.1°±0.6° (2.0°–6.0°)#,†

*$p < 0.0001$ compared to intact

#$p < 0.05$ compared to intact

†$p < 0.05$ compared to 4 rods

‡$p < 0.05$ compared to 2 rods + ALIF

Global lumbar range of motion with instrumentation

Table 3 demonstrates ROM of the entire L1–S1 segment for the intact specimen and the four instrumented configurations.

When comparing the intact specimen to instrumented configurations in flexion–extension, the average ROM decreased by 94% with 2 rods (2R and 2R + ALIF) and by 96% with 4 rods (4R and 4R + ALIF, respectively). The decrease in ROM was significant for each configuration ($p < 0.0001$). The average ROM was 2.5° with 2R and 2.8° with 2R + ALIF, whereas ROM was 1.9° with 4R and 4R + ALIF, respectively. When comparing the influence of the number of rods, 4-rod configurations reduced the ROM slightly but significantly compared to 2-rod configurations: 2R versus 4R ($p = 0.035$), 4R versus 2R + ALIF ($p = 0.010$), 4R + ALIF versus 2R + ALIF ($p = 0.002$). There was no significant difference between 2R and 2R + ALIF ($p = 0.444$) and between 4R and 4R + ALIF ($p = 0.756$).

In lateral bending, average ROM ranged between 1.2° and 1.5° and each configuration reduced ROM by 96% compared to the intact spine ($p < 0.0001$). There was no significant difference between the instrumented configurations.

In axial torsion, average ROM was decreased by 84% with 2R, by 87% with 4R and 4R + ALIF, respectively, and by 83% with 2R + ALIF compared to the intact spine ($p < 0.02$). When comparing the influence of number of rods and additional cage implantation, it appeared that 4 rods would mainly influence ROM: 2R versus 4R ($p = 0.066$), 4R versus 2R + ALIF ($p = 0.014$), 4R + ALIF versus 2R + ALIF ($p = 0.011$). There was no significant difference between 2R

and 2R + ALIF ($p = 0.361$) and between 4R and 4R + ALIF ($p = 0.957$).

Rod strain

Table 4 demonstrates average rod strain (RS) in the principal rods at the level L3–L4. There was no difference between left and right RS in any configuration.

When comparing 2- and 4-rod configurations in extension, 4R and 4R + ALIF decreased strain by 64% in the principal rods compared to 2R, respectively. In flexion, strain decreased by 68% with 4R and 65% with 4R + ALIF. For flexion and extension, the differences were significant between 2-rod and 4-rod configurations: 2R versus 4R ($p = 0.016$), 2R versus 4R + ALIF ($p = 0.015$), 2R + ALIF versus 4R ($p = 0.011$), 2R + ALIF versus 4R + ALIF ($p = 0.015$).

When analyzing the influence of cages with 2-rod configurations, it appeared that strain decreased by 1% in flexion with 2R + ALIF compared to 2R. In extension, cage implantation at L4–L5 and L5–S1 (2R + ALIF) increased strain by 22% at L3–L4 compared to 2R.

Discussion

Pseudarthrosis and rod fractures remain a major challenge in adult spinal deformity surgery since instrumentation to the sacrum and pelvis is often required. Daniels et al. [16] and Lertudomphonwanit et al. [24] analyzed risk factors for rod fractures and demonstrated that the patient's age, obesity, residual anterior malalignment, the number of instrumented levels, the use of osteotomies, the rod diameter and alloy might play a role. Four-rod instrumentation has been used recently to prevent pseudarthrosis and implant failure. Hyun et al. and Gupta et al. [18] compared radiologic outcomes after 2-rod and 4-rod instrumentation. These first clinical studies indicate that the incidence of pseudarthrosis is lower with 4-rod constructs and that revision surgery for rod

fractures was not required. However, long-term results are required to better understand the effects of this new instrumentation strategy. It seems that satellite rods limit minimal ROM and strain within principal rods, which could prevent rod fractures. Combining lumbosacral and pelvic instrumentation with interbody cages represents an additional strategy to prevent mechanical complications [25, 26]. Furthermore, Banno et al. [27] investigated the incidence of proximal pedicle and iliac screw loosening with 2-rod versus 4-rod constructs. A radiologic halo developed around screws in 21% of patients with 2-rod versus 33% after 4-rod instrumentation. This indicates that more rigid multiple rod instrumentations might lead to enhanced stress at the proximal and distal end of the construct. First studies on multiple rods focused on pedicle subtraction osteotomies (PSO). However, the exact role of additional cages remained unclear, and analyzing the scenario of adult scoliosis instrumentation without three-column osteotomies seemed mandatory.

Three-dimensional segmental ROM has been analyzed in vivo on lumbar spine radiographs of healthy volunteers [28–31]. These studies have demonstrated that the amount of ROM depends on the lumbar level. The highest ROM value in FE is located at L4–L5 and L5–S1. The largest ROM in LB and AT is located at L2–L3 and L3–L4. Panjabi et al. [32] studied segmental ROM from L1–L2 to L5–S1 in vitro and demonstrated results that were concordant with previous clinical radiographic findings. Guan et al. [33], Heuer et al. [34] and Charles et al. [35] studied L4–L5 ROM in vitro, and Hlubek et al. [36] reported normal values for L5–S1 ROM. Our results were in line with these previous findings, showing similar ROM corridors, when loading the entire lumbar spine up to 7.5 Nm.

Experimental cadaveric studies analyzing 4-rod posterior instrumentation can be found in the recent literature. However, most studies are based on PSO models [36–41]. Scheer et al. [37] compared multidirectional bending stiffness of multiple rod instrumentation with iliac fixation and L3 PSO in seven human spines (T11-pelvis). Satellite rods restored stiffness in FE and LB, but not in AT. The addition

Table 4 Maximum rod strain on the left and the right principal rods for each instrumentation in extension (−7.5 Nm) and flexion (7.5 Nm): average values ± standard deviation (minimum–maximum)

Configuration	Left		Right	
	Extension	Flexion	Extension	Flexion
2 rods	−0.026 ± 0.010 (−0.047 to −0.014)	0.027 ± 0.010 (0.017 to 0.047)	−0.025 ± 0.009 (−0.049 to −0.014)	0.027 ± 0.010 (0.014 to 0.054)
4 rods	−0.009 ± 0.003 (−0.012 to −0.007)[*,†]	0.009 ± 0.003 (0.006 to 0.013)[*,†]	−0.009 ± 0.003 (−0.013 to −0.005)[*,†]	0.009 ± 0.003 (0.006 to 0.013)[*,†]
4 rods + ALIF	−0.010 ± 0.003 (−0.013 to −0.007)[*,†]	0.009 ± 0.003 (0.008 to 0.013)[*,†]	−0.009 ± 0.003 (−0.012 to −0.004)[*,†]	0.009 ± 0.003 (0.005 to 0.014)[*,†]
2 rods + ALIF	−0.032 ± 0.012 (−0.054 to −0.015)	0.027 ± 0.010 (0.015 to 0.036)	−0.030 ± 0.011 (−0.058 to −0.013)	0.027 ± 0.010 (0.013 to 0.039)

*$p < 0.05$ compared to 2 rods

†$p < 0.05$ compared to 2 rods + ALIF

of cross-links restored stiffness in all bending modes including AT. The same study group further compared specimens with or without interbody cages above and below the L3 PSO. They showed that fatigue bending and dynamic stiffness increased by 22% after cage implantation in the segment L2–L4. Hallager et al. [38] assessed the effect of number of rods, alloys and anterior column support on ROM in five specimens (T12–S1) with a PSO at L3. All constructs significantly reduced ROM in FE and LB compared to intact (94.9–97.4%). Accessory rods mainly reduced FE motion, compared to 2-rod instrumentation. Furthermore, accessory rods reduced relative surface strain on the primary rods, and four CoCr rods with interbody cages above and below the PSO provided a 76% reduction in strain. La Barbera et al. [40] also tested seven human specimens (T12–S1) to assess the effect of multiple rods and cages in a PSO model. All construct types had a comparable effect in reducing global lumbar ROM compared to the intact spine (−94% in FE and LB; −80% in AT).

Strain is an index that can be used to predict rod failure. Hallager et al. [38] used uniaxial strain gauges and reported that accessory rods and CoCr rods reduced relative surface strain on primary rods, irrespective of the construct. The use of four CoCr rods and interbody cages provided 48% reduction in primary rod strain compared to 2-rod constructs. They reported a small decrease in primary and accessory rod strain at PSO level when adding interbody cages. Furthermore, strain was lower with CoCr compared to titanium rods. La Barbera et al. [40] used rosette gauges in a PSO model. When comparing 4-rod and 2-rod constructs, primary rod strain decreased by 74.4% in FE, 90.6% in LB and 63.5% in AR. This effect was enhanced when adding interbody cages. La Barbera et al. [41] described a similar effect in an anterior column realignment (ACR) model. The role of 4-rod constructs and interbody cages in reducing primary rod strain after PSO was further confirmed in finite element models [42–44]. Although the findings of these experimental settings focus on three-column osteotomies, the findings are in agreement with the results of our study, which represented a setting of lumbopelvic instrumentation for adult scoliosis. Godzik et al. [45] demonstrated that strain would increase in the caudal part of the construct when instrumenting the pelvis. Kleck et al. [46, 47] demonstrated that spinopelvic fixation increases L5–S1 rod strain especially during flexion. The addition of an ALIF divided strain by two in FE, but it had no effect in AT. Moreover, Hlubek et al. [36] investigated the effect of L5–S1 ALIF and transforaminal lumbar interbody fusion (TLIF) cages as well as iliac screws on rod and S1 pedicle screw strain. They demonstrated that iliac screws were protective of sacral screws but increased rod strain at L5–S1. When using iliac screws with 2 rods, the ALIF reduces rod strain significantly, whereas the TLIF did not. In our study strain gauges were placed at L3–L4, which represented the first level adjacent to a 360°

instrumentation (ALIF L4–L5 and L5–S1). Our findings suggested that the use of 2 rods with cages could increase rod strain in extension at the first adjacent level without cage. This is in line with the clinical findings of Lertudomphonwanit et al. [24] who showed that 44% of rod fractures occurred at L3–L4 when cages were implanted at L4–L5 and L5–S1. Our results indicated that 4 rods significantly decreased strain in primary rods at the adjacent level.

Although our findings provide a foundation for future clinical research with 4-rod constructs, some limitations are inherent to biomechanical studies. Standard lumbar loading conditions using pure moments up to 7.5 Nm were applied [23], although loading conditions for the entire lumbosacral spine might be revised for longer instrumentation configurations. Testing focused on the lumbosacral spine only, whereas scoliosis instrumentation usually involves thoracic segments as well. Moreover, rod strain measurement was analyzed at a single location in FE because of the use of uniaxial strain gauges, even if maximal strain and stress values could be located elsewhere. An additional analysis in LB and AR should be considered using rosette strain gauges in future studies. Nevertheless, such analysis with ROM and rod strain quantitative assessment provide a solid base for further finite element modeling and validation, thus yielding a deeper stress analysis in the entire spine construct to further complete the present results.

Conclusion

The results of this study indicate that using double rods and interbody cages can decrease residual ROM in FE and AT. The use of 4-rod constructs seemed to be the most efficient method in limiting strain in principal rods. The use of 2 rods with ALIF cages at L4–L5 and L5–S1 increases strain at L3–L4.

Compliance with ethical standards

Conflict of interest The authors declare that they have no conflict of interest.

References

1. Smith JS, Klineberg E, Schwab F, Shaffrey CI, Moal B, Ames CP, Hostin R, Fu KM, Burton D, Akbarnia B, Gupta M, Hart R, Bess S, Lafage V, International Spine Study Group (2013) Change in classification grade by the SRS-Schwab Adult Spinal Deformity Classification predicts impact on health-related quality of life

measures: prospective analysis of operative and nonoperative treatment. Spine (Phila Pa 1976) 38(19):1663–1671

2. Schwab FJ, Blondel B, Bess S, Hostin R, Shaffrey CI, Smith JS, Boachie-Adjei O, Burton DC, Akbarnia BA, Mundis GM, Ames CP, Kebaish K, Hart RA, Farcy JP, Lafage V, International Spine Study Group (ISSG) (2013) Radiographical spinopelvic parameters and disability in the setting of adult spinal deformity: a prospective multicenter analysis. Spine (Phila Pa 1976) 38(13):E803–E812

3. Kelly MP, Lenke LG, Bridwell KH, Agarwal R, Godzik J, Koester L (2013) Fate of the adult revision spinal deformity patient: a single institution experience. Spine (Phila Pa 1976) 38(19):E1196–E1200

4. Zhu F, Bao H, Liu Z, Bentley M, Zhu Z, Ding Y, Qiu Y (2014) Unanticipated revision surgery in adult spinal deformity: an experience with 815 cases at one institution. Spine (Phila Pa 1976) 39(26 Spec No.):B36–B44

5. Charosky S, Guigui P, Blamoutier A, Roussouly P, Chopin D (2012) Complications and risk factors of primary adult scoliosis surgery: a multicenter study of 306 patients. Spine (Phila Pa 1976) 37(8):693–700

6. Blamoutier A, Guigui P, Charosky S, Roussouly P, Chopin D (2012) Surgery of lumbar and thoracolumbar scolioses in adults over 50. Morbidity and survival in a multicenter retrospective cohort of 180 patients with a mean follow-up of 4.5 years. Orthop Traumatol Surg Res 98(5):528–535

7. Riouallon G, Bouyer B, Wolff S (2016) Risk of revision surgery for adult idiopathic scoliosis: a survival analysis of 517 cases over 25 years. Eur Spine J 25(8):2527–2534

8. Volkheimer D, Reichel H, Wilke H-J, Lattig F (2017) Is pelvic fixation the only option to provide additional stability to the sacral anchorage in long lumbar instrumentation? A comparative biomechanical study of new techniques. Clin Biomech Bristol Avon 43:34–39

9. Schwab FJ, Hawkinson N, Lafage V, Smith JS, Hart R, Mundis G, Burton DC, Line B, Akbarnia B, Boachie-Adjei O, Hostin R, Shaffrey CI, Arlet V, Wood K, Gupta M, Bess S, Mummaneni PV, International Spine Study Group (2012) Risk factors for major peri-operative complications in adult spinal deformity surgery: a multi-center review of 953 consecutive patients. Eur Spine J 21(12):2603–2610

10. Yamato Y, Matsuyama Y, Hasegawa K, Aota Y, Akazawa T, Iida T, Ueyama K, Uno K, Kanemura T, Kawakami N, Kotani T, Takaso M, Takahashi J, Tanaka M, Taneichi H, Tsuji T, Hosoe H, Mochida J, Shimizu T, Yonezawa I, Watanabe K, Matsumoto M, Committee for Adult Deformity, Japanese Scoliosis Society (2017) A Japanese nationwide multicenter survey on perioperative complications of corrective fusion for elderly patients with adult spinal deformity. J Orthop Sci 22(2):237–242

11. Vaz K, Verma K, Protopsaltis T, Schwab F, Lonner B, Errico T (2010) Bone grafting options for lumbar spine surgery: a review examining clinical efficacy and complications. SAS J 4(3):75–86

12. Mummaneni PV, Dhall SS, Eck JC, Groff MW, Ghogawala Z, Watters WC, Dailey AT, Resnick DK, Choudhri TF, Sharan A, Wang JC, Kaiser MG (2014) Guideline update for the performance of fusion procedures for degenerative disease of the lumbar spine. Part 11: interbody techniques for lumbar fusion. J Neurosurg Spine 21(1):67–74

13. Mobbs RJ, Phan K, Malham G, Seex K, Rao PJ (2015) Lumbar interbody fusion: techniques, indications and comparison of interbody fusion options including PLIF, TLIF, MI-TLIF, OLIF/ATP, LLIF and ALIF. J Spine Surg 1(1):2–18

14. Hyun S-J, Lenke LG, Kim Y-C, Koester LA, Blanke KM (2014) Comparison of standard 2-rod constructs to multiple-rod constructs for fixation across 3-column spinal osteotomies. Spine (Phila Pa 1976) 39(22):1899–1904

15. Merrill RK, Kim JS, Leven DM, Kim JH, Cho SK (2017) Multi-rod constructs can prevent rod breakage and pseudarthrosis at the lumbosacral junction in adult spinal deformity. Glob Spine J 7(6):514–520

16. Daniels AH, DePasse JM, Durand W, Hamilton DK, Passias P, Kim HJ, Protopsaltis T, Reid DBC, LaFage V, Smith JS, Shaffrey C, Gupta M, Klineberg E, Schwab F, Burton D, Bess S, Ames C, Hart RA, International Spine Study Group (2018) Rod fracture after apparently solid radiographic fusion in adult spinal deformity patients. World Neurosurg 117:e530–e537

17. Guevara-Villazón F, Boissiere L, Hayashi K, Larrieu D, Ghailane S, Vital J-M, Gille O, Pointillart V, Obeid I, Bourghli A (2020) Multiple-rod constructs in adult spinal deformity surgery for pelvic-fixated long instrumentations: an integral matched cohort analysis. Eur Spine J 29(4):886–895

18. Gupta S, Eksi MS, Ames CP, Deviren V, Durbin-Johnson B, Smith JS, Gupta MC (2018) A novel 4-rod technique offers potential to reduce rod breakage and pseudarthrosis in pedicle subtraction osteotomies for adult spinal deformity correction. Oper Neurosurg (Hagerstown) 14(4):449–456

19. Humbert L, De Guise JA, Aubert B, Godbout B, Skalli W (2009) 3D reconstruction of the spine from biplanar X-rays using parametric models based on transversal and longitudinal inferences. Med Eng Phys 31(6):681–687

20. Mitton D, Deschênes S, Laporte S, Godbout B, Bertrand S, de Guise JA, Skalli W (2006) 3D reconstruction of the pelvis from bi-planar radiography. Comput Methods Biomech Biomed Eng 9(1):1–5

21. Ghostine B, Sauret C, Assi A, Bakouny Z, Khalil N, Skalli W, Ghanem I (2017) Influence of patient axial malpositioning on the trueness and precision of pelvic parameters obtained from 3D reconstructions based on biplanar radiographs. Eur Radiol 27(3):1295–1302

22. Muth-seng C, Brauge D, Soriau N, Sandoz B, Van den Abbeele M, Skalli W, Laporte S (2019) Experimental analysis of the lower cervical spine in flexion with a focus on facet tracking. J Biomech 93:220–225

23. Wilke HJ, Wenger K, Claes L (1998) Testing criteria for spinal implants: recommendations for the standardization of in vitro stability testing of spinal implants. Eur Spine J Off Publ Eur Spine Soc Eur Spinal Deform Soc Eur Sect Cerv Spine Res Soc 7(2):148–154

24. Lertudomphonwanit T, Kelly MP, Bridwell KH, Lenke LG, McAnany SJ, Punyarat P, Bryan TP, Buchowski JM, Zebala LP, Sides BA, Steger-May K, Gupta MC (2018) Rod fracture in adult spinal deformity surgery fused to the sacrum: prevalence, risk factors, and impact on health-related quality of life in 526 patients. Spine J 18(9):1612–1624

25. La Barbera L, Galbusera F, Wilke H-J, Villa T (2016) Preclinical evaluation of posterior spine stabilization devices: can the current standards represent basic everyday life activities? Eur Spine J 25(9):2909–2918

26. La Barbera L, Galbusera F, Wilke H-J, Villa T (2017) Preclinical evaluation of posterior spine stabilization devices: can we compare in vitro and in vivo loads on the instrumentation? Eur Spine J 26(1):200–209

27. Banno T, Hasegawa T, Yamato Y, Togawa D, Yoshida G, Kobayashi S, Yasuda T, Arima H, Oe S, Mihara Y, Ushirozako H, Matsuyama Y (2019) Multi-rod constructs can increase the incidence of iliac screw loosening after surgery for adult spinal deformity. Asian Spine J 13(3):500–510

28. Pearcy M, Portek I, Shepherd J (1984) Three-dimensional X-ray analysis of normal movement in the lumbar spine. Spine (Phila Pa 1976) 9(3):294–297

29. Pearcy MJ, Tibrewal SB (1984) Axial rotation and lateral bending in the normal lumbar spine measured by three-dimensional radiography. Spine (Phila Pa 1976) 9(6):582–587

30. Dvorák J, Panjabi MM, Chang DG, Theiler R, Grob D (1991) Functional radiographic diagnosis of the lumbar spine. Flexion-extension and lateral bending. Spine (Phila Pa 1976) 16(5):562–571

31. Hayes MA, Howard TC, Gruel CR, Kopta JA (1989) Roentgenographic evaluation of lumbar spine flexion-extension in asymptomatic individuals. Spine (Phila Pa 1976) 14(3):327–331

32. Panjabi MM, Oxland TR, Yamamoto I, Crisco JJ (1994) Mechanical behavior of the human lumbar and lumbosacral spine as shown by three-dimensional load-displacement curves. J Bone Joint Surg Am 76(3):413–424

33. Guan Y, Yoganandan N, Moore J, Pintar FA, Zhang J, Maiman DJ, Laud P (2007) Moment–rotation responses of the human lumbosacral spinal column. J Biomech 40(9):1975–1980

34. Heuer F, Schmidt H, Klezl Z, Claes L, Wilke H-J (2007) Stepwise reduction of functional spinal structures increase range of motion and change lordosis angle. J Biomech 40(2):271–280

35. Charles YP, Persohn S, Steib J-P, Mazel C, Skalli W (2011) Influence of an auxiliary facet system on lumbar spine biomechanics. Spine (Phila Pa 1976) 36(9):690–699

36. Hlubek RJ, Godzik J, Newcomb AGUS, Lehrman JN, de Andrada B, Bohl MA, Farber SH, Kelly BP, Turner JD (2019) Iliac screws may not be necessary in long-segment constructs with L5–S1 anterior lumbar interbody fusion: cadaveric study of stability and instrumentation strain. Spine J 9(5):942–950

37. Scheer JK, Tang JA, Deviren V, Buckley JM, Pekmezci M, McClellan RT, Ames CP (2011) Biomechanical analysis of revision strategies for rod fracture in pedicle subtraction osteotomy. Neurosurgery 69(1):164–172

38. Hallager DW, Gehrchen M, Dahl B, Harris JA, Gudipally M, Jenkins S, Wu AM, Bucklen BS (2016) Use of supplemental short pre-contoured accessory rods and cobalt chrome alloy posterior rods reduces primary rod strain and range of motion across the pedicle subtraction osteotomy level: an in vitro biomechanical study. Spine (Phila Pa 1976) 41(7):E388–E395

39. Dahl BT, Harris JA, Gudipally M, Moldavsky M, Khalil S, Bucklen BS (2017) Kinematic efficacy of supplemental anterior lumbar interbody fusion at lumbosacral levels in thoracolumbosacral deformity correction with and without pedicle subtraction osteotomy at L3: an in vitro cadaveric study. Eur Spine J 26(11):2773–2781

40. La Barbera L, Brayda-Bruno M, Liebsch C, Villa T, Luca A, Galbusera F, Wilke HJ (2018) Biomechanical advantages of supplemental accessory and satellite rods with and without interbody cages implantation for the stabilization of pedicle subtraction osteotomy. Eur Spine J 27(9):2357–2366

41. La Barbera L, Wilke H-J, Liebsch C, Villa T, Luca A, Galbusera F, Brayda-Bruno M (2020) Biomechanical in vitro comparison between anterior column realignment and pedicle subtraction osteotomy for severe sagittal imbalance correction. Eur Spine J 29(1):36–44

42. Seyed Vosoughi A, Joukar A, Kiapour A, Parajuli D, Agarwal AK, Goel VK, Zavatsky J (2019) Optimal satellite rod constructs to mitigate rod failure following pedicle subtraction osteotomy (PSO): a finite element study. Spine J 19(5):931–941

43. Luca A, Ottardi C, Lovi A, Brayda-Bruno M, Villa T, Galbusera F (2017) Anterior support reduces the stresses on the posterior instrumentation after pedicle subtraction osteotomy: a finite-element study. Eur Spine J 26(Suppl 4):450–456

44. Luca A, Ottardi C, Sasso M, Prosdocimo L, La Barbera L, Brayda-Bruno M, Galbusera F, Villa T (2017) Instrumentation failure following pedicle subtraction osteotomy: the role of rod material, diameter, and multi-rod constructs. Eur Spine J 26(3):764–770

45. Godzik J, Hlubek RJ, Newcomb AGUS, Lehrman JN, de Andrada Pereira B, Farber SH, Lenke LG, Kelly BP, Turner JD (2019) Supplemental rods are needed to maximally reduce rod strain across the lumbosacral junction with TLIF but not ALIF in long constructs. Spine J 19(6):1121–1131

46. Kleck CJ, Illing D, Lindley EM, Noshchenko A, Patel VV, Barton C, Baldini T, Cain CMJ, Burger EL (2017) Strain in posterior instrumentation resulted by different combinations of posterior and anterior devices for long spine fusion constructs. Spine Deform 5(1):27–36

47. Kleck CJ, Illing D, Lindley EM, Noshchenko A, Patel VV, Barton C, Baldini T, Cain CMJ, Burger EL (2018) Reply to Letter to Editor: strain in posterior instrumentation resulted by different combinations of posterior and anterior devices for long spine fusion constructs. Spine Deform 6(3):335–340